Antonie van Leeuwenhoek (2020) 113:1737–1750
https://doi.org/10.1007/s10482-019-01366-5

ORIGINAL PAPER

Rhodopirellula heiligendammensis sp. nov., *Rhodopirellula pilleata* sp. nov., and *Rhodopirellula solitaria* sp. nov. isolated from natural or artificial marine surfaces in Northern Germany and California, USA, and emended description of the genus *Rhodopirellula*

Nicolai Kallscheuer · Sandra Wiegand · Mareike Jogler · Christian Boedeker · Stijn H. Peeters · Patrick Rast · Anja Heuer · Mike S. M. Jetten · Manfred Rohde · Christian Jogler

Received: 25 July 2019 / Accepted: 25 November 2019 / Published online: 4 December 2019

Abstract Expanding the collection of Planctomycetes by characterisation of novel species is key to better understanding of their complex lifestyles, uncommon cell biology and unexplored metabolism. Here, we isolated three novel planctomycetal strains from a kelp forest on the California Coastline at Monterey Bay or from plastic surfaces submerged in the Baltic Sea and the estuary of the river Warnow in the northeast of Germany. According to our phylogenetic analysis, the isolated strains Poly21^T, Pla100^T and CA85^T represent three novel species within the genus *Rhodopirellula*. All three show typical planctomycetal traits such as division by budding. All are aerobic, mesophilic chemoheterotrophs and show genomic features comparable to other described *Rhodopirellula* species. However, strain CA85^T is exceptional as it forms cream colonies, but no aggregates, which is a notable deviation from the pink- to red-pigmented and aggregate-forming *Rhodopirellula* species known thus far. We propose the names *Rhodopirellula heiligendammensis* sp. nov., *Rhodopirellula pilleata* sp. nov., and *Rhodopirellula solitaria* sp. nov. for the novel strains Poly21^T (DSM 102266^T = LMG 29467^T = CECT 9847^T = VKM B-3435^T), Pla100^T (DSM 102937^T = LMG 29465^T) and CA85^T (DSM 109595^T = LMG 29699^T = VKM B-3451^T), respectively, which we present as the respective type strains of these novel species.

Keywords Marine bacteria · Planctomycetes · *Rhodopirellula* · Baltic Sea · Kelp forest · Microplastic particles · Monterey Bay

N. Kallscheuer · S. Wiegand · M. Jogler · S. H. Peeters · M. S. M. Jetten · C. Jogler (✉)
Department of Microbiology, Radboud University, Nijmegen, The Netherlands
e-mail: christian@jogler.de

M. Jogler · C. Boedeker · P. Rast · A. Heuer
Leibniz Institute DSMZ, Brunswick, Germany

M. Rohde
Helmholtz Centre for Infection Research, Brunswick, Germany

Introduction

Planctomycetes are ubiquitous microorganisms often found in aquatic environments. They are Gram-negative bacteria that belong to the PVC (Planctomycetes–Verrucomicrobia–Chlamydiae) superphylum (Spring et al. 2016; Wagner and Horn 2006). The phylum Planctomycetes itself is divided into the classes *Phycisphaerae* and *Planctomycetia* (and *Candidatus* Brocadiae). The order *Planctomycetales* is currently the only validly described order within the class *Planctomycetia* and is further subdivided into

three families, namely *Planctomycetaceae*, *Isosphaeraceae* and *Gemmataceae*, to which the vast majority of described planctomycetal species belong.

In order to survive in oligotrophic 'deserts' such as seawater, species of the family *Planctomycetaceae* have been shown to attach to many different biotic surfaces (Bengtsson et al. 2012; Bondoso et al. 2015, 2014, 2017; Vollmers et al. 2017). For this purpose, many perform a lifestyle switch between planktonic swimming daughter and sessile mother cells (Jogler et al. 2011). In particular, species of the genus *Rhodopirellula* are believed to be potent degraders of polymeric sugars released from algal surfaces (Jeske et al. 2013; Wegner et al. 2013). A large set of glycolytic enzymes such as sugar hydrolases, esterases, deacylases and sulfatases encoded in their genomes supports the hypothesis that such species are capable of using naturally-occurring complex sugars or other highly decorated compounds as carbon and energy sources (Ivanova et al. 2017; Wallner et al. 2005; Wegner et al. 2013). Unique pili-forming crateriform structures and an enlarged periplasm are likely involved in the uptake and probably also cleavage of such compounds (Boedeker et al. 2017). Such a unique uptake mechanism allows the intracellular degradation of high molecular weight carbon sources. This could be a decisive advantage compared to extracellular cleavage by secreted enzymes, a strategy that would provide easily accessible carbon sources also to competing microorganisms occupying the same ecological niches (Frank et al. 2014; Wiegand et al. 2018).

Several members of the family *Planctomycetaceae* are predominant in biofilms on marine biotic surfaces (Bengtsson and Øvreås 2010; Kohn et al. 2019), which is rather unexpected when considering that many planctomycetal strains grow considerably slower than most of their natural competitors. Earlier studies revealed the presence of several *Rhodopirellula* species in European coastal sediments (Žure et al 2015). Sediments close to Sylt Island in the North Sea were investigated, a location which is quite close to the isolation source of *Rhodopirellula baltica*, the first *Rhodopirellula* species, isolated from brackish water of Kiel Fjord in the Baltic Sea (Schlesner et al. 2004). In addition to the specialised machinery for the uptake of polymeric compounds, production of metabolites with anti-microbial or anti-oxidative activity might also explain the observed planctomycetal predominance (Kallscheuer et al. 2019c). This notion is supported by their large genomes, e.g. of *Rhodopirellula* species, and predicted gene clusters involved in small molecule production (Graca et al. 2016; Jeske et al. 2016). The presence of unusual giant genes might correlate with small molecule production as well (Faria et al. 2018; Kohn et al. 2016; Wiegand et al. 2019).

Not only metabolically, but also structurally, Planctomycetes have been found to possess exceptional traits compared to canonical bacteria. Many of those, such as the lack of peptidoglycan (König et al. 1984), a compartmentalised cell plan (Lindsay et al. 1997), a nucleus-like structure (Fuerst and Webb 1991) and performance of endocytosis (Lonhienne et al. 2010) did however not prove to be verifiable. With the exception of *Candidatus* Brocadiaceae (Jogler 2014; Neumann et al. 2014), the proposed compartments turned out to be invaginations of the cytoplasmic membrane (Acehan et al. 2013; Boedeker et al. 2017). Also, the presence of peptidoglycan in Planctomycetes was confirmed (Jeske et al. 2015; van Teeseling et al. 2015). Such findings contributed to the reinterpretation of the cell plan of Planctomycetes as Gram-negative (Boedeker et al. 2017; Devos 2014). Nonetheless, Planctomycetes remain exceptional in comparison to well-characterised bacteria of other phyla, *e.g.* due to the lack of canonical divisome proteins including FtsZ (Jogler et al. 2012; Pilhofer et al. 2008) and an unusual mode of division, either by budding, binary fission or even alternation of both modes (Wiegand et al. 2018, 2019). The unique and highly diverse biology of Planctomycetes is a driving force for expanding the collection of planctomycetal strains, which is prerequisite for getting a better insight into their physiology.

Here, we describe three novel planctomycetal strains isolated from a kelp forest on the California Coastline at Monterey Bay or from plastic surfaces submerged in the Baltic Sea and the estuary of the river Warnow in the northeast of Germany.

Materials and methods

Isolation of the novel strains

The strains were isolated as described before (Wiegand et al. 2019). Briefly, for isolation of Poly21^T and

Pla100^T, incubators containing polyethylene particles were stored for two weeks at different locations in Northern Germany: Poly21^T was isolated on 8 October 2015 from an incubator placed at a depth of 2 m below Heiligendamm pier (Seebrücke Heiligendamm) (exact location 54.146 N 11.843 E). Pla100^T was isolated on 4 September 2014 from an incubator placed in the Unterwarnow, the estuary of the Warnow river located in the city of Rostock (sampling location 54.106 N 12.096 E), close to a wastewater treatment plant discharge. The exact setup of sampling was described in detail earlier (Oberbeckmann et al. 2018). CA85^T was isolated on 28 November 2014 from leaves of a giant bladder kelp (*Macrocystis pyrifera*) on the Californian coastline in Monterey Bay, CA, USA (36.619 N 121.901 W). Kelp pieces were initially washed with 100 mg/L cycloheximide dissolved in sterile-filtered natural seawater to prevent fungal growth, then swabbed over M1H *N*-acetyl glucosamine (NAG) artificial seawater (ASW) media plates containing 8 g/L gellan gum, 1000 mg/L streptomycin, 200 mg/L ampicillin and 20 mg/L cycloheximide and incubated at 20 °C for two to three weeks.

Cultivation conditions

After isolation, the strains were cultivated in M1 medium with 4-(2-hydroxyethyl)-1-piperazineethanesulfonic acid (HEPES) as buffering agent and additionally supplemented with ASW and NAG. Designation of the final medium is M1H NAG ASW and it was prepared as previously described (Kallscheuer et al. 2019a).

Light and electron microscopy

Phase contrast (Phaco) analyses and field emission scanning electron microscopy were performed according to a previously published protocol (Kallscheuer et al. 2019a).

Genome information

Genome information of the three isolated strains is available from GenBank under accession numbers SJPU00000000 (Poly21^T), SJPM00000000 (Pla100^T) and SJPK00000000 (CA85^T). 16S rRNA gene sequences are available from GenBank under accession numbers MK554550 (Poly21^T), MK554546 (Pla100^T) and MK554540 (CA85^T). Methods used for DNA isolation and genome sequencing were described before (Wiegand et al. 2019).

Phylogenetic analysis

16S rRNA gene phylogeny was computed for strains Pla100^T, CA85^T and Poly21^T, the type strains of all described planctomycetal species (as of May 2019) and all isolates recently published (Wiegand et al. 2019) and validly named (Boersma et al. 2019; Kallscheuer et al. 2019a, b, d; Kohn et al. 2019). The 16S rRNA gene sequences were aligned with SINA (Pruesse et al. 2012) and the phylogenetic inference was calculated with RAxML (Stamatakis 2014) with a maximum likelihood (ML) approach with 1000 bootstraps, nucleotide substitution model GTR, gamma distributed rate variation and estimation of proportion of invariable sites (GTRGAMMAI option). Three 16S rRNA genes of bacterial strains from the PVC superphylum were used as outgroup. The *average nucleotide identity* (ANI) was calculated using OrthoANI (Lee et al. 2016). *Average amino acid identity* (AAI) was calculated using the aai.rb script of the enveomics collection (Rodriguez-R and Konstantinidis 2016) and the *percentage of conserved proteins* (POCP) was calculated as described (Qin et al. 2014). The *rpoB* nucleotide sequences were taken from the above-mentioned genomes as well as other publicly available genome annotations and the sequence identities were determined as described (Bondoso et al. 2013). Upon extracting only those parts of the sequence that would have been sequenced with the described primer set the alignment and matrix calculation was performed with Clustal Omega (Sievers et al. 2011). For the multi-locus sequence analysis (MLSA) the unique single-copy core genome of all analysed genomes was determined with proteinortho5 (Lechner et al. 2011) with the 'selfblast' option enabled. The protein sequences of the resulting orthologous groups were aligned using MUSCLE v.3.8.31 (Edgar 2004). After clipping, partially aligned *C*- and *N*-terminal regions and poorly aligned internal regions were filtered using Gblocks (Castresana 2000). The final alignment was concatenated and clustered using the maximum likelihood method implemented by RaxML (Stamatakis 2014) with the

"rapid bootstrap" method and 500 bootstrap replicates.

Results and discussion

Phylogenetic analysis

The phylogenetic inference of the novel isolates shows that the three strains Poly21^T, Pla100^T and CA85^T cluster monophyletically within the recently emended genus *Rhodopirellula* (Kallscheuer et al. 2019c) (Fig. 1). The 16S rRNA gene identity of the three isolated strains and the type species *R. baltica* SH1^T lies between 95.7% and 96.3%, which is above the genus threshold of 94.5% (Yarza et al. 2014) (Table 1, Fig. 2). The indicated proposal of the novel isolates belonging to the *Rhodopirellula* genus is also supported by POCP values > 50% against *R. baltica* SH1^T (Qin et al. 2014) (Table 1). The AAI analysis gave values of 58.7–59.2% (Table 1). These values are somewhat below the proposed AAI genus threshold of 60–80%, but nevertheless well within the ranges found for other bacterial genera (Luo et al. 2014), thereby also allowing the novel isolates an affiliation to the genus *Rhodopirellula*.

The last criterion for the affiliation to the genus *Rhodopirellula* is the *rpoB* sequence identity of Poly21^T, Pla100^T and CA85^T compared to *R. baltica* SH1^T of 79.8%, 82.0% and 79.0%, respectively. Values in this range are above the genus threshold (Kallscheuer et al. 2019d) (Table 1). The *rpoB* sequence identities < 95.5% (Fig. 1 and Table 1) also confirm that the novel isolates form separate species

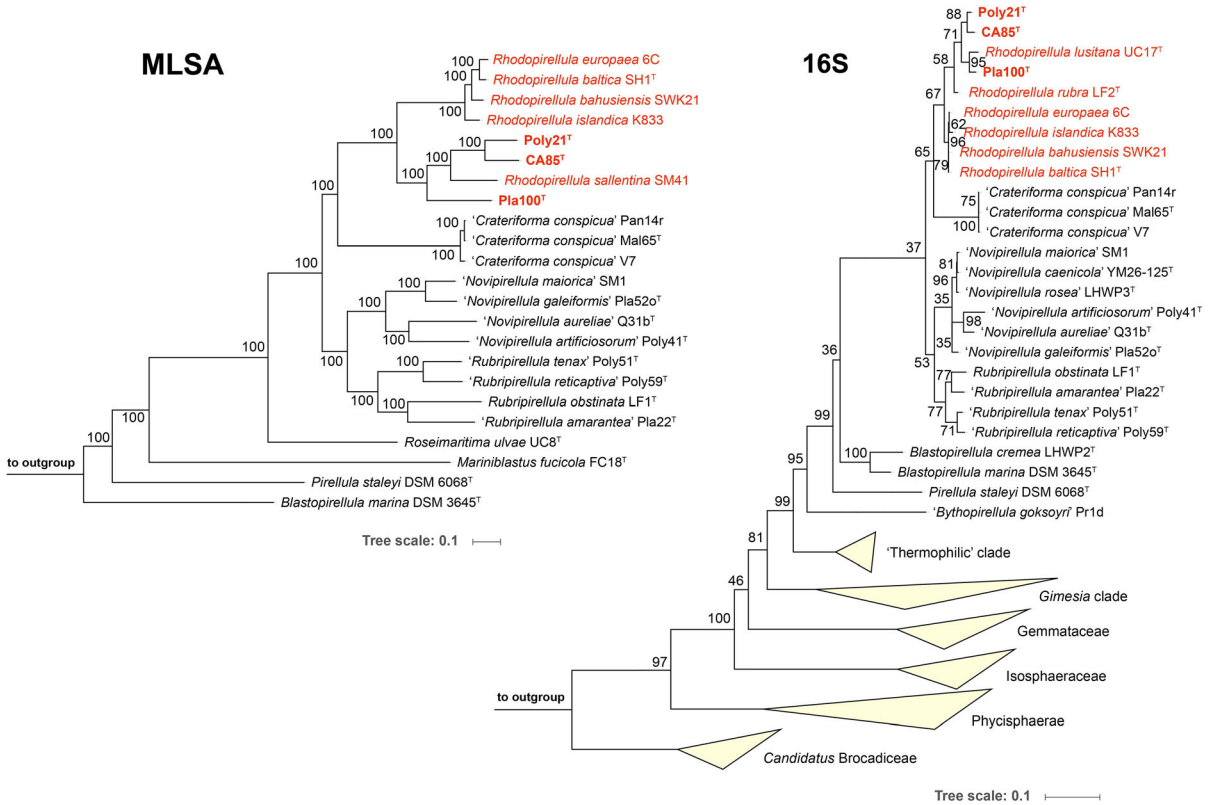

Fig. 1 Maximum likelihood phylogenetic analysis. Phylogenetic trees showing the position of the three novel strains Pla100^T, CA85^T and Poly21^T. Recently described species are included (Kallscheuer et al. 2019b, d). 16S rRNA gene- and MLSA-based phylogeny was computed as described in the Material and Methods section. The outgroup consists of three 16S rRNA genes from the PVC superphylum. In the MLSA-based tree *Bythopirellula goksoyri* Pr1d served as outgroup. The *Gimesia* clade includes species of the genera *Gimesia*, *Planctopirus*, *Fuerstiella*, *Schlesneria*, *Rubinisphaera* and *Planctomicrobium*, while the thermophilic clade includes species of the genus *Thermostilla*, *Thermogutta* and *Thermopirellula*

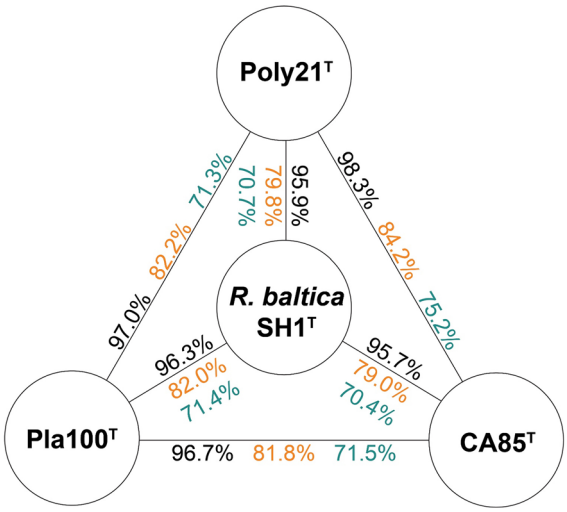

Fig. 2 Similarity values of the novel isolates Poly21^T, Pla100^T and CA85^T in relation to type species *Rhodopirellula baltica* SH1^T. The black font gives the 16S rRNA gene identity, the orange font gives the *rpoB* sequence identity and the turquoise font the whole genome-based *average nucleotide identity* (ANI)

within the genus *Rhodopirellula*. The same can be shown by the comparison of the ANI, as all values are clearly below the species threshold of 95–96% (Kim et al. 2014) and by 16S rRNA gene identities below the species threshold of 98.7% (Stackebrandt and Ebers 2006) (Fig. 2).

Genomic characteristics

The genomes of strains Poly21^T (7.1 Mb) and CA85^T (6.8 Mb) are similar in size, whereas Pla100^T has a larger genome (8.5 Mb). The genome sizes are in the same range as for closely related species, e.g. *R. baltica* (7.1 Mb), *Rhodopirellula bahusiensis* (7.8 Mb) and *Rhodopirellula sallentina* (8.2 Mb). Detailed genomic characteristics data for the novel strains in comparison to the type species *R. baltica* SH1^T are summarised in Table 2. The most striking difference when comparing the three isolated strains is the number of tRNAs. Pla100^T harbours 114 tRNA genes, while the number is between 40 and 55 in the other two strains and 91 in *R. baltica*. CA85^T harbours two copies of the 16S rRNA-encoding gene, while only single copies are present in the other three strains. The G + C content of the genomes is between 55 and 58%, which is in the same range as observed for previously characterised *Rhodopirellula* species.

Morphology and physiology

We analysed the cell morphology of strains Poly21^T, Pla100^T and CA85^T employing light microscopy (LM, Fig. 3) and scanning electron microscopy (SEM, Fig. 4). For this purpose, cells were cultivated in M1H NAG ASW medium and harvested during the exponential growth phase.

Cells of strain Poly21^T are pear-shaped to round with an average size of 2.4 ± 0.3 µm in length and 1.9 ± 0.2 µm in width (Fig. 3a, c). Colonies have a coral pink colour. Poly21^T cells form loose aggregates. Cell division is performed by polar budding with the daughter cell having the same shape as the mother cell (Fig. 3a). The strain is aerobic and grows at pH values ranging from 5.5 to 9.0 (Fig. 5). An optimal growth at pH 8.5 suggests that strain Poly21^T is slightly alkaliphilic. Growth was observed at temperatures ranging from 10 to 33 °C with optimal growth at 30 °C (Fig. 5). In M1H NAG ASW medium

Table 1 Similarity values of the novel isolates Poly21^T, Pla100^T and CA85^T and the described *Rhodopirellula species*

Species name	16S rRNA	POCP	AAI	*rpoB*	ANI
Rhodopirellula baltica SH1^T	100	100	100	100	100
CA85^T	95.7	57.4	59.2	79.0	70.4
Pla100^T	96.3	60.2	58.7	82.0	71.4
Poly21^T	95.9	57.5	59.0	79.8	70.7
Rhodopirellula europaea 6C	99.9	80.9	88.5	95.7	88.7
Rhodopirellula sallentina SM41	97.7	57.8	58.6	81.8	71.5
Rhodopirellula islandica K833	99.5	77.3	82.0	89.7	81.7
Rhodopirellula lusitana UC17^T	96.3	n.a	n.a	n.a	n.a
Rhodopirellula rubra LF2^T	97.5	n.a	n.a	n.a	n.a
Rhodopirellula bahusiensis SWK21	100	n.a	n.a	n.a	n.a

The similarity values in percent are given for each strain compared to the type species *Rhodopirellula baltica* SH1^T

n.a. not available

Table 2 Phenotypic and genotypic features of strains Pla100^T, CA85^T and Poly21^T compared to *Rhodopirellula baltica* SH1^T

Characteristics	Poly21^T	Pla100^T	CA85^T	*R. baltica* SH1^T
Phenotypic features				
Size	2.4 × 1.9 µm	2.2 × 1.0 µm	2.0 × 1.3 µm	1.0–2.5 × 1.2–2.3 µm
Colour	Coral pink	Brink pink	Cream	Pink
Shape	Ovoid to pear-shaped	Elongated pear-shaped	Pear-shaped	Ovoid to pear-shaped
Aggregates	Yes	Yes	No	Yes
Division	Budding	Budding	Budding	Budding
Flagella	n.o.	Yes	n.o.	Yes
Crateriform structures	n.o.	n.o.	n.o.	Yes
Fimbriae	Polar matrix or fiber	Polar matrix or fiber	Overall matrix or fiber	Polar matrix or fiber
Capsule	n.o.	n.o.	n.o.	n.o.
Bud shape	Like mother cell	Slimmer than mother cell	Like mother cell	Like mother cell
Stalk	n.o.	n.o.	n.o.	no
Holdfast structure	n.o.	n.o.	n.o.	yes
Genotypic features				
Genome size [bp]	7,177,699	8,502,319	6,796,955	7,145,576
Plasmids [bp]	n.o.	n.o	n.o.	n.o.
GC [%]	56.5 ± 2.4	55.8 ± 1.5	58.0 ± 2.8	55.4
Completeness [%]	96.39	98.28	98.28	98.28
Contamination [%]	1.72	0	1.72	1.72
Protein-coding genes	5696	6194	5227	5569
Hypothetical proteins	2573	2697	2362	3078
Protein-coding genes/Mb	794	729	769	764
Coding density [%]	88.2	88.6	86.7	88.7
16S rRNA genes	1	1	2	1
tRNA genes	52	114	45	91

n.o. not observed

a maximal growth rate of 0.064 h^{-1} was observed, which corresponds to a doubling time of approximately 11 h.

Colonies of strain Pla100^T have a similar colour as Poly21^T but the cell shape is different (Table 2). In contrast to Poly21^T, Pla100^T cells have an elongated shape, which becomes obvious when comparing the cells sizes of both strains. Although similar in length (Poly21^T: 2.4 µm, Pla100^T: 2.3 µm), cell width of Pla100^T (1.0 µm) is only half of the width of Poly21^T (1.9 µm) (Figs. 3c, h, 4c). Strain Pla100^T divides by budding with the bud being slimmer than the mother cell. Stronger aggregate formation of Pla100^T compared to Poly21^T was observed, which is also reflected in the formation of a polar extracellular matrix by strain Pla100^T. Pla100^T grows at a pH range of 5.5 to 8.5 (optimum 7.0) and a temperature range of 10–33 °C (optimum 30 °C) (Fig. 5). The maximal observed growth rate of Pla100^T was 0.033 h^{-1}, which is approximately half of the growth rate of Poly21^T, thus the doubling time of Pla100^T is 21 h.

The third strain, CA85^T, has a cell size of 2.0 µm × 1.3 µm and is slightly smaller than Poly21^T, but similar in shape. Although producing an extracellular matrix covering the entire cell surface (Fig. 4f), CA85^T did not form aggregates (Fig. 4e). Instead, individual cells were observed during SEM and light microscopy. Cells divide by budding (Fig. 3g). Strain CA85^T reached a maximal growth rate of 0.066 h^{-1} (generation time: 11 h), which is very similar to that obtained for Poly21^T. The strain grew in the same pH and temperature range as Pla100^T with optimal growth at pH 7.5 and 27 °C (Fig. 5). Some characteristics of CA85^T are exceptional

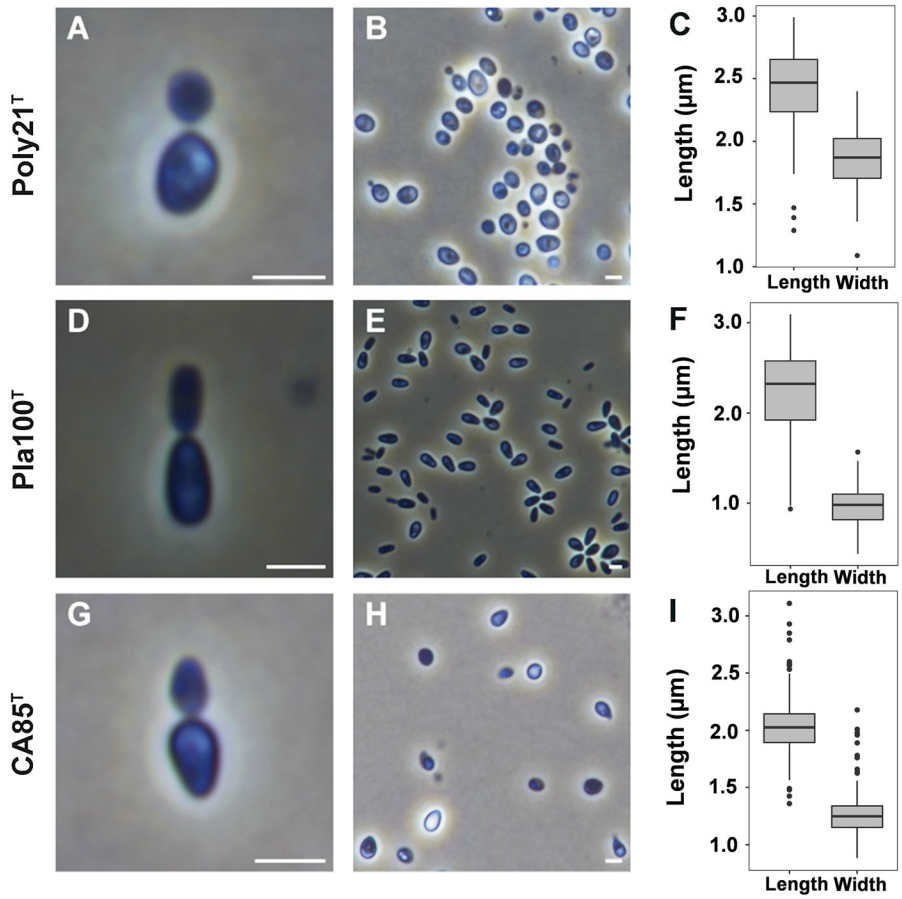

Fig. 3 Light microscopy images and cell size plots of strains Pla100^T, CA85^T and Poly21^T. The mode of cell division (**a**, **c**, **e**) and a general overview of cell morphology (**b**, **d**, **f**) is shown in the pictures. The scale bar is 1 µm. For determination of the cell size (**g**, **h**, **i**) at least 100 representative cells were counted manually or by using a semi-automated object count tool

compared to other *Rhodopirellula* species. CA85^T forms cream colonies and is the first known *Rhodopirellula* strain not showing a pink or red pigmentation. Additionally, the lack of aggregate formation is also a major difference to most of the *Rhodopirellula* species characterised thus far. Basic aspects of morphology and mechanism of cell division for all strains are summarised in Table 2.

Based on the genome sequences we analysed key metabolic capabilities in the primary and secondary metabolism of the three strains in comparison to *R. baltica* SH1^T. In our analysis, we focused on the central carbon metabolism comprising glycolytic pathways, pentose phosphate pathway, citric acid cycle (TCA cycle), gluconeogenesis and anaplerotic reactions, such as the glyoxylate shunt (Table 3). Obtained results suggest that all four strains use the Embden–Meyerhof–Parnas pathway for the degradation of sugars as we were able to assign genes to all required enzymatic reactions of this most common glycolytic pathway. The absence of additional glycolytic pathways, e.g. the Entner–Doudoroff pathway, was reinforced by the absence of 2-dehydro-3-deoxyphosphogluconate aldolase in all four strains. The pentose phosphate pathway also appears to be functional in all four strains. This was to some extent expected as important precursors for the biosynthesis of L-histidine, the three aromatic amino acids and nucleotides are provided by this pathway. All enzymes of the TCA cycle are encoded, however, growth of *Rhodopirellula* species with acetate or fatty acids as sole carbon and energy source appears unlikely as all

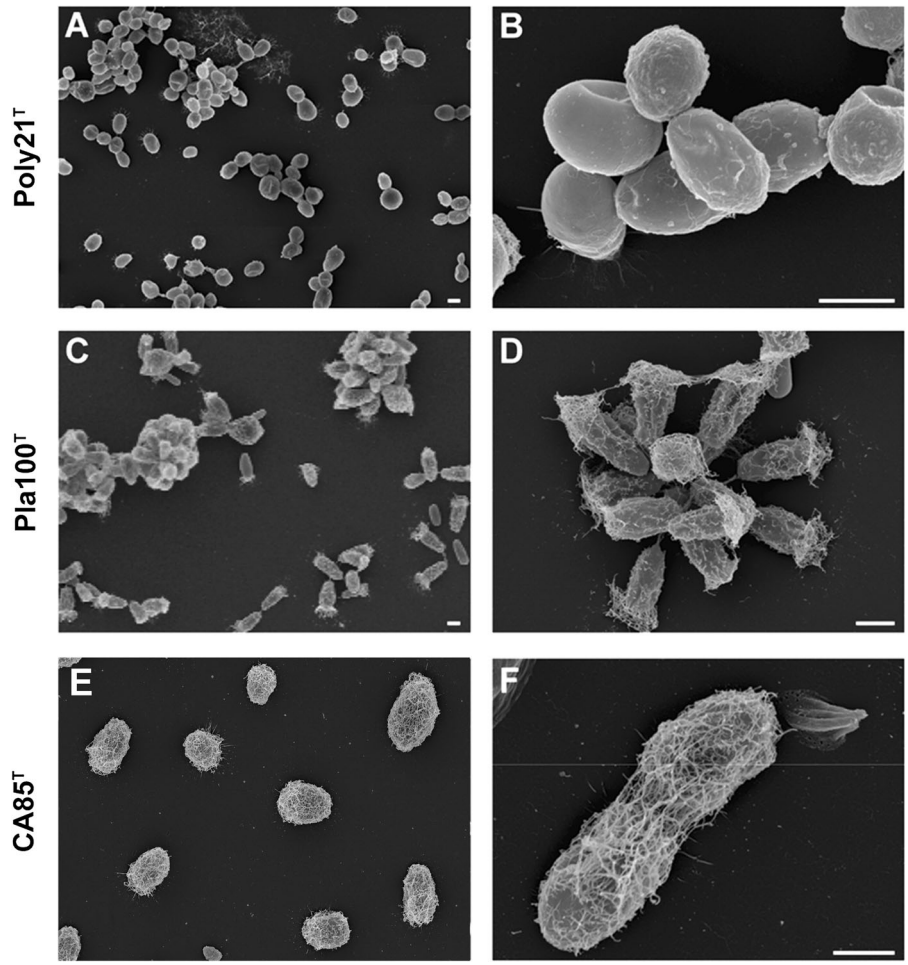

Fig. 4 Scanning electron microscopic pictures of the three novel strains Pla100^T, CA85^T and Poly21^T. The scale bar is 1 μm

four strains lack the glyoxylate shunt enabling anaplerosis during growth on the above-mentioned carbon sources. Remarkably, key gluconeogenic enzymes also seem to be absent in the four strains. This further supports the prediction that *Rhodopirellula* species are unable to use acetate or e.g. TCA cycle intermediates as sole carbon and energy source since an incomplete gluconeogenesis would not allow for production of sugars, which are essential for biosynthesis of cell wall components. Taken together, our analysis leads to the hypothesis that the metabolism of the here analysed *Rhodopirellula* strains is rather adapted to sugars as substrates for biomass formation and does not seem to support good growth with short- or long-chain carboxylic acids.

To gain a first insight into the potential for secondary metabolite biosynthesis an AntiSMASH analysis was performed (Blin et al. 2019). Here, we focused on terpenoid-forming proteins, polyketide synthases (PKS) and non-ribosomal peptide synthetases (NRPS) as these enzyme classes are known to be responsible for production of bioactive small molecules (Table 4). It is likely that Planctomycetes follow other, yet uncharacterised, pathways for secondary metabolite production, however these will most likely escape the AntiSMASH prediction. In the genomes of the three strains isolated here, 6–9 clusters potentially involved in small molecule production were found. This number is comparable to *R. baltica* SH1^T (six clusters). The distribution of the clusters into different types of PKSs, NRPSs, mixed PKS-NRPSs and terpenoid-forming clusters is similar, but not identical. All four species have in common the lack of type II PKSs, and presence of one type III PKS and

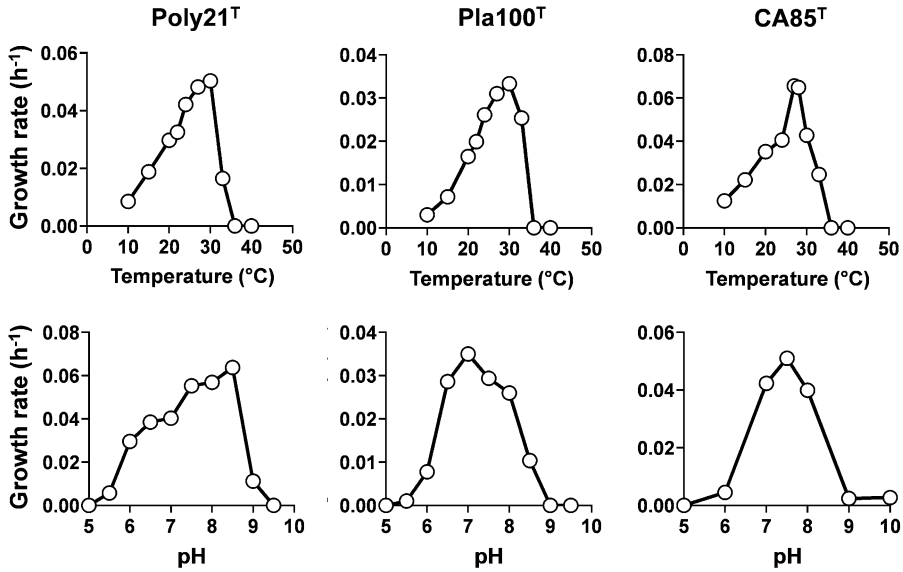

Fig. 5 Temperature and pH optima of the isolated strains Pla100^T, CA85^T and Poly21^T**.** The graphs show the average growth rates obtained from cultivation of the three isolated strains in M1H NAG ASW medium in biological triplicates. Cultivations at different pH values were conducted at 28 °C and cultivations at different temperatures were performed at pH 7.5

two terpenoid clusters. *R. baltica* lacks an NRPS-encoding cluster, while one putative NRPS was identified in the three novel isolates. The number of clusters correlated with the genome size of the strains. The genome of Pla100^T is around 20% larger than the genome of the other three strains and this strain also contains the highest number of clusters.

Conclusion

Based on our physiological and phylogenetic analyses, we conclude that the three characterised strains represent three novel species within the genus *Rhodopirellula*. Thus, we propose the names *Rhodopirellula heiligendammensis* sp. nov., *Rhodopirellula pilleata* sp. nov., and *Rhodopirellula solitaria* sp. nov. with strains Poly21^T, Pla100^T and CA85^T as the respective type strains of these novel species.

Description of *Rhodopirellula heiligendammensis* sp. nov.

Rhodopirellula heiligendammensis (hei.li.gen.dam.-men'sis. N.L. fem. adj. *heiligendammensis* of Heiligendamm; referring to the origin of the bacterium from Heiligendamm, Germany).

Cells are pear-shaped to round (length: 2.4 ± 0.3 μm, width: 1.9 ± 0.2 μm), form aggregates and divide by polar budding. Cells grow at 10–33 °C (optimum 30 °C) and at pH 5.5–9.0 (optimum 8.5). Colonies are coral pink. The genome sequence (acc. no. SJPU00000000) and 16S rRNA gene sequence (acc. no. MK554550) of the type strain are available from GenBank. The type strain is Poly21^T (DSM 102266^T = LMG 29467^T = CECT 9847^T = VKM B-3435^T), isolated from polyethylene particles incubated in 2 m depth in the Baltic Sea close to Heiligendamm, Germany in October 2015.

Description of *Rhodopirellula pilleata* sp. nov.

Rhodopirellula pilleata (pil.le.a'ta. L. fem. adj. *pilleata* wearing a headgear; referring to the hat-like shape of the fibers).

Cells are elongated pear-shaped (length: 2.3 ± 0.4 μm, width: 1.0 ± 0.2 μm), form aggregates and divide by budding. Colonies are brink pink. The temperature optimum is 30 °C (growth observed from 10–33 °C). Growth is observed at pH 5.5–8.5 (optimum 7.0). The genome sequence (acc. no. SJPM00000000) and 16S rRNA gene sequence (acc. no. MK554546) of the type strain are available from GenBank. The type strain is Pla100^T (DSM

Table 3 Genome-based primary metabolism of the isolated strains compared to *Rhodopirellula baltica* SH1^T

Enzyme/reaction	EC number	gene	SH1^T	Pla100^T	CA85^T	Poly21^T
Glycolysis						
Glucose-6-phosphate isomerase	5.3.1.9	*pgi*	y	Pla100_49290	CA85_00640	Poly21_23760
ATP-dependent 6-phosphofructokinase isozyme 1	2.7.1.11	*pfkA*	y	Pla100_36530	CA85_47860	Poly21_09990
Fructose-bisphosphate aldolase class 2	4.1.2.13	*fbaA*	y	Pla100_10300	CA85_19670	Poly21_22920
Triosephosphate isomerase	5.3.1.1	*tpiA*	y	Pla100_29890	CA85_45830	Poly21_14990
Glyceraldehyde-3-phosphate dehydrogenase	1.2.1.12	*gapA*	y	Pla100_17980	CA85_18640	Poly21_51860
Phosphoglycerate kinase	2.7.2.3	*pgk*	y	Pla100_01510	CA85_20620	Poly21_35120
2,3-bisphosphoglycerate-independent phosphoglycerate mutase	5.4.2.12	*gpmI*	y	Pla100_56880	CA85_31560	Poly21_13360
Enolase	4.2.1.11	*eno*	y	Pla100_44690	CA85_36170	Poly21_43900
Pyruvate kinase I	2.7.1.40	*pykF*	y	Pla100_02430	CA85_30320	Poly21_37930
Pyruvate dehydrogenase E1 component	1.2.4.1	*aceE*	y	Pla100_39510	CA85_23840	Poly21_05800
Dihydrolipoyllysine-residue acetyltransferase component of pyruvate dehydrogenase complex	2.3.1.12	*aceF*	y	Pla100_39520	CA85_23850	Poly21_05810
Gluconeogenesis						
Phosphoenolpyruvate carboxylase	4.1.1.31	*ppc*	y	Pla100_28760	n	n
Pyruvate, phosphate dikinase	2.7.9.1	*ppdK*	y	Pla100_48270	CA85_34090	Poly21_02900
Phosphoenolpyruvate carboxykinase (ATP)	4.1.1.49	*pckA*	n	n	n	n
Phosphoenolpyruvate carboxykinase [GTP]	4.1.1.32	*pckG*	n	n	n	n
Fructose-1,6-bisphosphatase class 2	3.1.3.11	*glpX*	n	n	n	n
Fructose-1,6-bisphosphatase class 1	3.1.3.11	*fbp*	n	n	n	n
Pyrophosphate–fructose 6-phosphate 1-phosphotransferase	2.7.1.90	*pfp*	n	n	n	n
Pentosephosphate pathway						
Glucose-6-phosphate 1-dehydrogenase	1.1.1.49	*zwf*	y	Pla100_59190	CA85_00560	Poly21_22840
6-phosphogluconolactonase	3.1.1.31	*pgl*	y	Pla100_09630	CA85_32360	Poly21_06780
				Pla100_00220	CA85_47300	Poly21_09460
6-phosphogluconate dehydrogenase, decarboxylating	1.1.1.44	*gndA*	y	Pla100_47270	CA85_15360	Poly21_45790
Transketolase 2	2.2.1.1	*tktB*	y	Pla100_34370	CA85_34360	Poly21_08820
Transaldolase B	2.2.1.2	*talB*	y	Pla100_44630	CA85_11980	Poly21_41310
Entner–Doudoroff pathway						
2-dehydro-3-deoxy-phosphogluconate aldolase	4.1.2.14	*eda*	n	n	n	n
Phosphogluconate dehydratase	4.2.1.12	*edd*	y	Pla100_33810	CA85_30430	Poly21_14460
				Pla100_47340	CA85_42150	Poly21_09960
				Pla100_07380	CA85_16750	Poly21_03610
TCA cycle						
Citrate synthase	2.3.3.16	*gltA*	y	Pla100_34250	CA85_26680	Poly21_34540
Aconitate hydratase A	4.2.1.3	*acnA*	y	Pla100_62570	CA85_38500	Poly21_36490
Isocitrate dehydrogenase [NADP]	1.1.1.42	*icd*	y	Pla100_02930	CA85_25480	Poly21_36170
2-oxoglutarate dehydrogenase E1 component	1.2.4.2	*sucA*	y	Pla100_42890	CA85_29660	Poly21_37910
Dihydrolipoyllysine-residue succinyltransferase component of 2-oxoglutarate dehydrogenase complex	2.3.1.61	*sucB*	y	Pla100_30350	CA85_10780	Poly21_37490
Succinate–CoA ligase [ADP-forming] subunit alpha	6.2.1.5	*sucD*	y	Pla100_13480	CA85_27450	Poly21_12060
Succinate–CoA ligase [ADP-forming] subunit beta	6.2.1.5	*sucC*	y	Pla100_13490	CA85_27460	Poly21_12050
Succinate dehydrogenase flavoprotein subunit	1.3.5.1	*sdhA*	y	Pla100_34220	CA85_26710	Poly21_34510

Table 3 continued

Enzyme/reaction	EC number	gene	SH1^T	Pla100^T	CA85^T	Poly21^T
Succinate dehydrogenase iron-sulfur subunit	1.3.5.1	*sdhB*	y	Pla100_34210	CA85_26720	Poly21_34500
Succinate dehydrogenase cytochrome b556 subunit	1.3.5.1	*sdhC*	y	Pla100_34230	CA85_26700	Poly21_34520
Succinate dehydrogenase hydrophobic membrane anchor subunit	1.3.5.1	*sdhD*	n	n	n	n
Fumarate hydratase class I, an/aerobic	4.2.1.2	*fumA/B*	n	n	n	n
Fumarate hydratase class II	4.2.1.2	*fumC*	y	Pla100_08050	CA85_14610	Poly21_49100
Malate dehydrogenase	1.1.1.37	*mdh*	y	Pla100_46850	CA85_17390	Poly21_45440
				Pla100_46460	CA85_15310	Poly21_45710
					CA85_24870	
Glyoxylate shunt						
Isocitrate lyase	4.1.3.1	*aceA*	n	n	n	n
Malate synthase G	2.3.3.9	*glcB*	n	n	n	n

Presence of a gene in SH1^T is indicated by 'y' and absence is indicated by 'n'. The analysis is based on genome sequences with the following accession numbers: NC_005027.1 (*R. baltica* SH1^T), SJPM00000000 (Pla100^T), CA85^T (SJPK00000000) and Poly21^T (SJPU00000000)

Table 4 Numbers of genetic clusters putatively involved in secondary metabolite production

	Terpenoid	Type I PKS	Type II PKS	Type III PKS	Type I PKS-NRPS	NRPS	Total
R. baltica SH 1^T	2	2	0	1	1	0	6
Poly21^T	2	3	0	1	0	1	7
CA85^T	2	2	0	1	0	1	6
Pla100^T	2	3	0	1	2	1	9

102937^T = LMG 29465^T), isolated from polyethylene particles submerged in the Unterwarnow close to a wastewater treatment plant discharge in Rostock, Germany in September 2014.

Description of *Rhodopirellula solitaria* sp. nov.

Rhodopirellula solitaria (sol.i.ta'ri.a. L. fem. adj. *solitaria* lonely; referring to the solitary occurrence of the cells and the absence of aggregates).

Cells are pear-shaped (2.0 ± 0.3 × 1.3 ± 0.2 µm) and divide by budding. Colonies have a cream colour. Preferred temperature and pH are 27 °C and 7.5, respectively, while growth is observed in the range of 10–33 °C and at pH 6.0–8.5. The genome sequence (acc. no. SJPK00000000) and 16S rRNA gene sequence (acc. no. MK554540) of the type strain are available from GenBank. The type strain is CA85^T (DSM 109595^T = LMG 29699^T = VKM B-3451^T), isolated from a giant bladder kelp (*M. pyrifera*) in a kelp forest in Monterey Bay, CA, USA in November 2014.

Emended description of the genus *Rhodopirellula* Schlesner et al. 2004

The description of the genus *Rhodopirellula* is as given previously (Schlesner et al. 2004), with the following modification: Colony colours range from cream to pink. Crateriform structures are not always present.

Acknowledgements Part of this research was funded by the Deutsche Forschungsgemeinschaft Grants KA 4967/1-1 and JO 893/4-1, Grant ALWOP.308 of the Nederlandse Organisatie voor Wetenschappelijk Onderzoek (NWO), SIAM (Soehngen Institute for Anaerobic Microbiology) Grant No. 024002002 and the Radboud Excellence fellowship. We thank Ina Schleicher for skillful technical assistance. Brian Tindall and Regine Fähnrich from the DSMZ as well as the BCCM/LMG Bacteria collection we thank for support during strain deposition. We thank Anne-Kristin Kaster (KIT Karlsruhe, Germany) and Alfred M. Spormann (Stanford, USA) as well as the Aquarius Dive Shop Monterey and the Hopkins Marine Station for sampling support. We also thank our collaborators Sonja Oberbeckmann and Matthias Labrenz (IOW Warnemünde, Germany) for support during sampling.

Author contributions NK wrote the manuscript and analysed the cultivation data. SW performed the genomic and phylogenetic analysis. AH, PR and MJ isolated the strains and performed the initial cultivation and strain deposition. SHP and CB performed the light microscopic analysis and prepared the LM pictures. MSMJ contributed to text preparation and revised the manuscript. MR performed the electron microscopic analysis and prepared the SEM pictures. CJ took the samples and supervised the study. All authors read and approved the final version of the manuscript.

Compliance with ethical standards

Conflict of interest The authors declare that they have no conflict of interest.

Ethical statement This article does not contain any studies with animals performed by any of the authors.

References

Acehan D, Santarella-Mellwig R, Devos DP (2013) A bacterial tubulovesicular network. J Cell Sci 127:277–280

Bengtsson MM, Øvreås L (2010) Planctomycetes dominate biofilms on surfaces of the kelp *Laminaria hyperborea*. BMC Microbiol 10:261

Bengtsson MM, Sjøtun K, Lanzén A, Øvreås L (2012) Bacterial diversity in relation to secondary production and succession on surfaces of the kelp *Laminaria hyperborea*. ISME J 6:2188–2198

Blin K, Shaw S, Steinke K, Villebro R, Ziemert N, Lee SY, Medema MH, Weber T (2019) AntiSMASH 5.0: updates to the secondary metabolite genome mining pipeline. Nucleic Acids Res 47:W81–W87

Boedeker C, Schuler M, Reintjes G, Jeske O, van Teeseling MC, Jogler M, Rast P, Borchert D, Devos DP, Kucklick M, Schaffer M, Kolter R, van Niftrik L, Engelmann S, Amann R, Rohde M, Engelhardt H, Jogler C (2017) Determining the bacterial cell biology of Planctomycetes. Nat Commun 8:14853

Boersma A, Kallscheuer N, Wiegand S, Rast R, Peeters S, Mesman R, Heuer A, Boedeker C, Jetten M, Rohde M, Jogler M (2019) *Alienimonas californiensis* gen. nov. sp. nov., a novel Planctomycete isolated from the kelp forest in Monterey Bay. Antonie van Leeuwenhoek. https://doi.org/10.1007/s10482-019-01367-4

Bondoso J, Harder J, Lage OM (2013) *rpoB* gene as a novel molecular marker to infer phylogeny in *Planctomycetales*. Antonie Van Leeuwenhoek 104:477–488

Bondoso J, Balague V, Gasol JM, Lage OM (2014) Community composition of the Planctomycetes associated with different macroalgae. FEMS Microbiol Ecol 88:445–456

Bondoso J, Albuquerque L, Nobre MF, Lobo-da-Cunha A, da Costa MS, Lage OM (2015) *Roseimaritima ulvae* gen. nov., sp. nov. and *Rubripirellula obstinata* gen. nov., sp. nov. two novel planctomycetes isolated from the epiphytic community of macroalgae. Syst Appl Microbiol 38:8–15

Bondoso J, Godoy-Vitorino F, Balague V, Gasol JM, Harder J, Lage OM (2017) Epiphytic Planctomycetes communities associated with three main groups of macroalgae. FEMS Microbiol Ecol 93:fiw255

Castresana J (2000) Selection of conserved blocks from multiple alignments for their use in phylogenetic analysis. Mol Biol Evol 17:540–552

Devos DP (2014) Re-interpretation of the evidence for the PVC cell plan supports a gram-negative origin. Antonie Van Leeuwenhoek 105:271–274

Edgar RC (2004) MUSCLE: multiple sequence alignment with high accuracy and high throughput. Nucleic Acids Res 32:1792–1797

Faria M, Bordin N, Kizina J, Harder J, Devos D, Lage OM (2018) Planctomycetes attached to algal surfaces: insight into their genomes. Genomics 110:231–238

Frank O, Michael V, Pauker O, Boedeker C, Jogler C, Rohde M, Petersen J (2014) Plasmid curing and the loss of grip—the 65-kb replicon of *Phaeobacter inhibens* DSM 17395 is required for biofilm formation, motility and the colonization of marine algae. Syst Appl Microbiol 38:120–127

Fuerst JA, Webb RI (1991) Membrane-bounded nucleoid in the eubacterium *Gemmata obscuriglobus*. Proc Natl Acad Sci USA 88:8184–8188

Graca AP, Calisto R, Lage OM (2016) Planctomycetes as novel source of bioactive molecules. Front Microbiol 7:1241

Ivanova AA, Naumoff DG, Miroshnikov KK, Liesack W, Dedysh SN (2017) Comparative genomics of four Isosphaeraceae planctomycetes: a common pool of plasmids and glycoside hydrolase genes shared by *Paludisphaera borealis* PX4^T, *Isosphaera pallida* IS1B^T, *Singulisphaera acidiphila* DSM 18658^T, and strain SH-PL62. Front Microbiol 8:412

Jeske O, Jogler M, Petersen J, Sikorski J, Jogler C (2013) From genome mining to phenotypic microarrays: Planctomycetes as source for novel bioactive molecules. Antonie Van Leeuwenhoek 104:551–567

Jeske O, Schüler M, Schumann P, Schneider A, Boedeker C, Jogler M, Bollschweiler D, Rohde M, Mayer C, Engelhardt H, Spring S, Jogler C (2015) Planctomycetes do possess a peptidoglycan cell wall. Nat Commun 6:7116

Jeske O, Surup F, Ketteniß M, Rast P, Förster B, Jogler M, Wink J, Jogler C (2016) Developing techniques for the utilization of Planctomycetes as producers of bioactive molecules. Front Microbiol 7:1242

Jogler C (2014) The bacterial 'mitochondrium'. Mol Microbiol 94:751–755

Jogler C, Glöckner FO, Kolter R (2011) Characterization of *Planctomyces limnophilus* and development of genetic tools for its manipulation establish it as a model species for the phylum Planctomycetes. Appl Environ Microbiol 77:5826–5829

Jogler C, Waldmann J, Huang X, Jogler M, Glöckner FO, Mascher T, Kolter R (2012) Identification of proteins likely to be involved in morphogenesis, cell division, and signal transduction in Planctomycetes by comparative genomics. J Bacteriol 194:6419–6430

Kallscheuer N, Jogler M, Wiegand S, Peeters S, Heuer A, Boedeker C, Jetten M, Rohde M, Jogler C (2019a) *Rubinisphaera italica* sp. nov. isolated from a hydrothermal area in the Tyrrhenian Sea close to the volcanic island Panarea. Antonie van Leeuwenhoek. https://doi.org/10.1007/s10482-019-01329-w

Kallscheuer N, Jogler M, Wiegand S, Peeters S, Heuer A, Boedeker C, Jetten M, Rohde M, Jogler C (2019b) Three novel *Rubripirellula* species isolated from artificial plastic surfaces submerged in the German part of the Baltic Sea and the estuary of the river Warnow. Antonie van Leeuwenhoek. https://doi.org/10.1007/s10482-019-01368-3

Kallscheuer N, Moreira C, Airs R, Llewellyn CA, Wiegand S, Jogler C, Lage OM (2019c) Pink-and orange-pigmented Planctomycetes produce saproxanthin-type carotenoids including a rare C45 carotenoid. Environ Microbiol Rep 11:741–748

Kallscheuer N, Wiegand S, Peeters SH, Jogler M, Boedeker C, Heuer A, Rast P, Jetten MSM, Rohde M, Jogler C (2019d) Description of three bacterial strains belonging to the new genus *Novipirellula* gen. nov., reclassificiation of *Rhodopirellula rosea* and *Rhodopirellula caenicola* and readjustment of the genus threshold of the phylogenetic marker *rpoB* for *Planctomycetaceae*. Antonie van Leeuwenhoek (accepted manuscript ANTO-D-19-00304)

Kim M, Oh HS, Park SC, Chun J (2014) Towards a taxonomic coherence between average nucleotide identity and 16S rRNA gene sequence similarity for species demarcation of prokaryotes. Int J Syst Evol Microbiol 64:346–351

Kohn T, Heuer A, Jogler M, Vollmers J, Boedeker C, Bunk B, Rast P, Borchert D, Glöckner I, Freese HM, Klenk HP, Overmann J, Kaster AK, Wiegand S, Rohde M, Jogler C (2016) *Fuerstia marisgermanicae* gen. nov., sp. nov., an unusual member of the phylum Planctomycetes from the German Wadden Sea. Front Microbiol 7:2079

Kohn T, Wiegand S, Boedeker C, Rast P, Heuer A, Jetten MSM, Schüler M, Becker S, Rohde C, Müller R-W, Brümmer F, Rohde M, Engelhardt H, Jogler M, Jogler C (2019) *Planctopirus ephydatiae*, a novel Planctomycete isolated from a freshwater sponge. Syst Appl Microbiol. https://doi.org/10.1016/j.syapm.2019.126022

König E, Schlesner H, Hirsch P (1984) Cell wall studies on budding bacteria of the *Planctomyces*/*Pasteuria* group and on a *Prosthecomicrobium* sp. Arch Microbiol 138:200–205

Lechner M, Findeiss S, Steiner L, Marz M, Stadler PF, Prohaska SJ (2011) Proteinortho: detection of (co-)orthologs in large-scale analysis. BMC Bioinform 12:124

Lee I, Ouk Kim Y, Park SC, Chun J (2016) OrthoANI: an improved algorithm and software for calculating average nucleotide identity. Int J Syst Evol Microbiol 66:1100–1103

Lindsay MR, Webb RI, Fuerst JA (1997) Pirellulosomes: a new type of membrane-bounded cell compartment in planctomycete bacteria of the genus *Pirellula*. Microbiol UK 143:739–748

Lonhienne TG, Sagulenko E, Webb RI, Lee KC, Franke J, Devos DP, Nouwens A, Carroll BJ, Fuerst JA (2010) Endocytosis-like protein uptake in the bacterium *Gemmata obscuriglobus*. Proc Natl Acad Sci USA 107:12883–12888

Luo C, Rodriguez RL, Konstantinidis KT (2014) MyTaxa: an advanced taxonomic classifier for genomic and metagenomic sequences. Nucleic Acids Res 42:e73

Neumann S, Wessels HJ, Rijpstra WI, Sinninghe Damste JS, Kartal B, Jetten MS, van Niftrik L (2014) Isolation and characterization of a prokaryotic cell organelle from the anammox bacterium *Kuenenia stuttgartiensis*. Mol Microbiol 94:794–802

Oberbeckmann S, Kreikemeyer B, Labrenz M (2018) Environmental factors support the formation of specific bacterial assemblages on microplastics. Front Microbiol 8:2709

Pilhofer M, Rappl K, Eckl C, Bauer AP, Ludwig W, Schleifer KH, Petroni G (2008) Characterization and evolution of cell division and cell wall synthesis genes in the bacterial phyla Verrucomicrobia, Lentisphaerae, Chlamydiae, and Planctomycetes and phylogenetic comparison with rRNA genes. J Bacteriol 190:3192–3202

Pruesse E, Peplies J, Glöckner FO (2012) SINA: accurate high-throughput multiple sequence alignment of ribosomal RNA genes. Bioinformatics 28:1823–1829

Qin Q-L, Xie B-B, Zhang X-Y, Chen X-L, Zhou B-C, Zhou J, Oren A, Zhang Y-Z (2014) A proposed genus boundary for the prokaryotes based on genomic insights. J Bacteriol 196:2210–2215

Rodriguez-R LM, Konstantinidis KT (2016) The enveomics collection: a toolbox for specialized analyses of microbial genomes and metagenomes. PeerJ Preprints 4:e1900v1

Schlesner H, Rensmann C, Tindall BJ, Gade D, Rabus R, Pfeiffer S, Hirsch P (2004) Taxonomic heterogeneity within the Planctomycetales as derived by DNA–DNA hybridization, description of *Rhodopirellula baltica* gen. nov., sp. nov., transfer of *Pirellula marina* to the genus *Blastopirellula* gen. nov. as *Blastopirellula marina* comb. nov. and emended description of the genus *Pirellula*. Int J Syst Evol Microbiol 54:1567–1580

Sievers F, Wilm A, Dineen D, Gibson TJ, Karplus K, Li W, Lopez R, McWilliam H, Remmert M, Söding J (2011) Fast, scalable generation of high-quality protein multiple sequence alignments using clustal omega. Mol Syst Biol 7:539

Spring S, Bunk B, Spröer C, Schumann P, Rohde M, Tindall BJ, Klenk H-P (2016) Characterization of the first cultured representative of Verrucomicrobia subdivision 5 indicates the proposal of a novel phylum. ISME J 10:2801

Stackebrandt E, Ebers J (2006) Taxonomic parameter revisited: tarnished gold standards. Microbiol Today 33:152–155

Stamatakis A (2014) RAxML version 8: a tool for phylogenetic analysis and post-analysis of large phylogenies. Bioinformatics 30:1312–1313

van Teeseling MC, Mesman RJ, Kuru E, Espaillat A, Cava F, Brun YV, Van Nieuwenhze MS, Kartal B, van Niftrik L (2015) Anammox Planctomycetes have a peptidoglycan cell wall. Nat Commun 6:6878

Vollmers J, Frentrup M, Rast P, Jogler C, Kaster AK (2017) Untangling genomes of novel planctomycetal and verrucomicrobial species from monterey bay kelp forest metagenomes by refined binning. Front Microbiol 8:472

Wagner M, Horn M (2006) The Planctomycetes, Verrucomicrobia, Chlamydiae and sister phyla comprise a superphylum with biotechnological and medical relevance. Curr Opin Biotechnol 17:241–249

Wallner SR, Bauer M, Würdemann C, Wecker P, Glöckner FO, Faber K (2005) Highly enantioselective *sec*-alkyl sulfatase activity of the marine planctomycete *Rhodopirellula baltica* shows retention of configuration. Angew Chem Int Ed Engl 44:6381–6384

Wegner C-E, Richter-Heitmann T, Klindworth A, Klockow C, Richter M, Achstetter T, Glöckner FO, Harder J (2013) Expression of sulfatases in *Rhodopirellula baltica* and the diversity of sulfatases in the genus *Rhodopirellula*. Mar Genomics 9:51–61

Wiegand S, Jogler M, Jogler C (2018) On the maverick Planctomycetes. FEMS Microbiol Rev 42:739–760

Wiegand S, Jogler M, Boedeker C, Pinto D, Vollmers J, Rivas-Marín E, Kohn T, Peeters SH, Heuer A, Rast P, Oberbeckmann S, Bunk B, Jeske O, Meyerdierks A, Storesund JE, Kallscheuer N, Lücker S, Lage OM, Pohl T, Merkel BJ, Hornburger P, Müller R-W, Brümmer F, Labrenz M, Spormann AM, Op den Camp HJM, Overmann J, Amann R, Jetten MSM, Mascher T, Medema MH, Devos DP, Kaster A-K, Øvreås L, Rohde M, Galperin MY, Jogler C (2019) Cultivation and functional characterization of 79 planctomycetes uncovers their unique biology. Nat Microbiol. https://doi.org/10.1038/s41564-019-0588-1

Yarza P, Yilmaz P, Pruesse E, Glöckner FO, Ludwig W, Schleifer KH, Whitman WB, Euzeby J, Amann R, Rossello-Mora R (2014) Uniting the classification of cultured and uncultured bacteria and archaea using 16S rRNA gene sequences. Nat Rev Microbiol 12:635–645

Žure M, Munn CB, Harder J (2015) Diversity of *Rhodopirellula* and related planctomycetes in a North Sea coastal sediment employing *carB* as molecular marker. FEMS Microbiol Lett 362:fnv127